Identification of Conformational Structures of 2-Phenylethanol and Its Singly Hydrated Complex by Mass Selective High-Resolution Spectroscopy and ab Initio Calculations†

Rosen Karaminkov, Sotir Chervenkov, and Hans J. Neusser*

Physikalische und Theoretische Chemie, Technische Universität München, Lichtenbergstrasse 4, D-85748 Garching, Germany

Received: August 14, 2007; In Final Form: October 19, 2007

The flexible prototype molecule 2-phenylethanol (2-PE) and its singly hydrated complex have been investigated in a cold supersonic beam by a combination of high-resolution two-color R2PI spectroscopy and quantum chemistry ab initio calculations. The existence of two monomer structures separated by a high potential energy barrier, gauche and anti ones, was proven. Higher energy conformers are supposed to relax to the observed ones during the jet expansion process. We have identified the conformational structure of the complex between 2-PE and water, which corresponds to water binding to the most stable gauche conformer. No detectable structural changes of the host 2-PE molecule have been observed upon attachment of a single water molecule. A conformational relaxation mechanism is suggested also for the 2-PE·H_2O complex.

I. Introduction

Many biological processes are regulated by relatively small, flexible molecules. A typical example for such molecules is neurotransmitters,[1,2] which play an important role in the human body. The properties and functionality of neurotransmitters depend significantly on their conformational structure, which is determined by a subtle interplay between weak intramolecular interactions and intermolecular interactions with the solvent. The importance of these interactions has been realized, and their detailed exploration has attracted a lot of scientific interest over the past decade. In recent investigations the combination of various spectroscopic techniques in the gas phase with advanced quantum chemistry computations has allowed the first retrieval of structural information on a number of neurotransmitters, including 2-phenylethylamine,[3−8] phenylalanine,[9] ephedrine,[10−12] norephedrine,[13] pseudoephedrine,[11] and adrenaline.[13]

2-Phenylethanol (2-PE) (see Scheme 1 with atom labels) is the hydroxy analogue of the neurotransmitter molecule 2-phenylethylamine. It has been extensively studied over the past years[5,7,14−19] as a neurotransmitter prototype molecule. The gauche structure of the most stable conformer of the 2-PE monomer has been conclusively established by microwave[15] and high-resolution resonant two-photon ionization (R2PI)[19] experiments combined with quantum chemistry ab initio calculations. Yet, however, there exist several unclear issues and controversies on the conformational structures of the bare molecule and the structure of its singly hydrated complex. The present work presents a detailed analysis of the existing conformers of the 2-PE monomer and discusses possible processes leading to interconversion of conformers in the jet expansion. The experimental findings from mass selective high-resolution UV two-photon resonance enhanced ionization spectroscopy of all pronounced bands in the vicinity of the strongest origin band are reconciled with the theoretical predictions on rotational constants, transition moment ratios, and vibrational frequencies from high-level ab initio quantum chemistry calculations. Through a confident assignment of all the observed vibronic bands in the vicinity of the strongest 0_0^0 origin band in the spectrum of the 2-PE monomer, we have concluded that two conformers, gauche and anti, are observed under the conditions of adiabatic expansion in a cold supersonic beam. The analysis of the theoretical potential energy surface corroborates the assumption that the higher energy conformers that presumably exist in the preexpansion region relax to the observed ones, with the latter being separated by a high potential barrier.

SCHEME 1: Atom Labels of the 2-PE·H_2O Complex

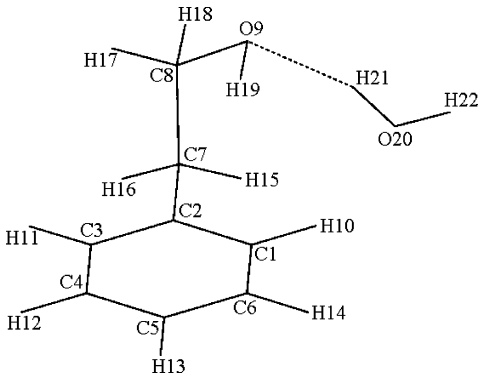

We also extended the study of 2-PE to its singly hydrated complex. This investigation renders itself as a natural extension of our previous study on the 2-PE·Ar complex,[19] where the structure is determined by the interplay between the intramolecular hydrogen bond and the intermolecular dispersion interactions. To our knowledge, this is the first application of mass resolved high-resolution UV spectroscopy to studying hydrated complexes of flexible biologically relevant molecules, which have been a subject of intense research in recent years.[18,20−25] The important issues addressed are whether and how solvent molecules affect the conformational structure of the flexible solute molecule and how the flexible molecule adapts its structure to the local environment under the combined action of intra- and intermolecular hydrogen bonds. Another interesting aspect is whether water stabilizes particular conformers, thus

† This work is dedicated to Prof. S.H. Lin on occasion of his 70th birthday.

* Corresponding author. Phone: +49 89 289 13 388. Fax: +49 89 289 13 412. E-mail: neusser@ch.tum.de.

10.1021/jp076541t CCC: $40.75
Published on Web 01/11/2008

acting as an efficient conformational selector. The complex between 2-PE and water is a prototype system for microsolvation and is expected to reveal the binding pattern and the influence of water on the conformational shape and stability of the host flexible molecule.

II. Experiment and Data Processing

The experimental setup used to measure the one- and two-color resonance enhanced two-photon ionization spectra of 2-PE has been described previously.[19,26−28] Briefly, the 2-PE vapor is mixed with Ar at a pressure of 3.0 bar and expanded into vacuum through a pulse-operated heatable nozzle with an orifice diameter of 300 μm. To increase the vapor concentration of 2-PE in the nozzle, the substance was heated to 96 °C. To reduce the Doppler broadening, a skimmer with an orifice of 1 mm in diameter is used. The molecular beam is intersected perpendicularly by two counterpropagating laser pulses. To obtain the one-color low-resolution spectrum, we used a tunable broad-band ($\Delta\nu \sim 0.4$ cm^{-1} full width at half-maximum (fwhm)) dye laser (Lambda Physik FL 2002) operated with Coumarin 153. The excitation scheme for producing the highly resolved two-color UV spectra employs two photons: one narrow-frequency excitation photon promotes the molecules from their ground, S_0, electronic state to the first excited, S_1, electronic state, and a second photon of fixed frequency provided by the above-mentioned broad-band dye laser ionizes the already excited molecules. The excitation photons are generated by frequency doubling in a BBO (beta barium borate) crystal of the pulsed amplified output of an Ar^+ ion laser (Coherent, Innova 400) pumped continuous wave single-mode ring dye laser (Coherent, CR 699-21) operating with Coumarin 6 and generating laser radiation in the green wavelength range with 2 MHz full width at half-maximum (fwhm) line width and a power of up to 250 mW. The produced narrow-band UV laser pulses have a nearly Fourier transform limited line width of 100 MHz (fwhm), and pulse duration of 10 ns (fwhm). The energy of the excitation photons is scanned over the rotational structure of selected vibronic bands of the $S_1 \leftarrow S_0$ transition. Both lasers are pumped by a XeCl excimer laser (Lambda Physik EMG 203) generating pulses at 308 nm with an energy of 240 mJ and a pulse duration of 20 ns (fwhm). The energies of the excitation and the ionization laser pulses after frequency doubling are up to 0.5 and 1.5 mJ, respectively. The ions are accelerated by the ion optics of a home-built Wiley−McLaren-type time-of-flight mass spectrometer and subsequently detected by microchannel plates whose output signal is integrated by a gated integrator. The absolute frequency is measured with an accurate wave meter (Atos 007, $\nu/\Delta\nu = 10^8$). The relative calibration of the measured spectra is performed by simultaneous recording of the fringe pattern of a confocal Fabry−Perot interferometer. The laser scan and the data acquisition are controlled by homemade software operating in the LabVIEW environment.

The analysis of the highly resolved spectra has been performed using our homemade rotational fit computer routine based on genetic algorithms.[19,29−31] Cross correlation was employed as a fitness function. The typical number of generations was 200 with 200 individuals in a generation.

III. Results

A. Low-Resolution Spectra. We have recorded low-resolution one-color resonant two-photon ionization (R2PI) spectra monitoring three different mass channels in the vicinity of the $S_1 \leftarrow S_0$ electronic transition of 2-PE under two different experimental conditions. In the first case, the spectrum was measured under water-free conditions by selecting the ion signal at the parent mass channel at $m/z = 122$. The spectrum is presented in Figure 1a. The 0_0^0 vibronic band and the small red-shifted band at 30 cm^{-1} have been discussed in our previous paper.[19] Here we discuss the blue-shifted vibronic features in the spectrum at +42, +48, +58, +136, and +213 cm^{-1}.

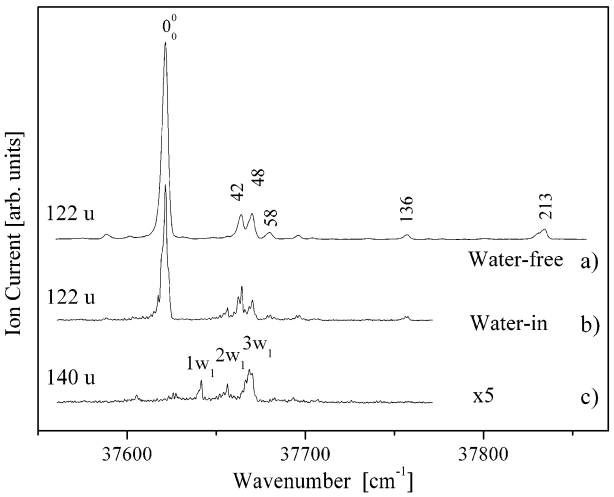

Figure 1. One-color R2PI spectra of the $S_1 \leftarrow S_0$ electronic transition of the 2-PE monomer measured at the monomer ($m/z = 122$) mass channel under water-free (a) and water-present (b) conditions, and of the 2-PE·H_2O complex (c) recorded at its parent ($m/z = 140$) mass channel.

The second set of spectra was recorded under water-in conditions monitoring both the parent mass channel at $m/z = 122$ and the mass channel of the singly hydrated 2-PE at $m/z = 140$. The two resulting spectra are shown in Figure 1b,c. The three most intense vibronic bands measured at the mass channel of the 2-PE−water cluster are labeled $1w_1$, $2w_1$, and $3w_1$, respectively. It has been found that the positions of peak +48 cm^{-1} in the monomer mass channel and peak $3w_1$ in the 2-PE−water cluster mass channel coincide. Therefore, peak +48 cm^{-1} is likely to originate from fragmentation of the 2-PE−water cluster. However, adding water does not change the relative intensity of this band. This leads us to the conclusion that $3w_1$ is a mixture of two close-lying bands: one of the 2-PE monomer and the other one of the 2-PE·H_2O complex. A clear evidence for the nature of this band is provided only by high-resolution spectroscopy, and is presented below. There is a stronger fragmentation behavior of band $2w_1$ in comparison with the other bands ($1w_1$ and $3w_1$) observed at this mass channel. This may be tentatively explained by the existence of 2-PE·H_2O cluster conformers of differing stability. The remaining smaller vibronic bands in the spectrum of Figure 1c measured at mass channel $m/z = 140$ do not correspond to any of the bands in Figure 1b measured at the mass channel of the monomer. As a next step, to elucidate the conformational structures giving rise to the above-described vibronic bands of 2-PE and its singly hydrated cluster, we measured the bands under discussion with a much higher resolution.

B. High-Resolution Spectra. *1. Monomer Bands.* The highly resolved UV spectra of all blue-shifted bands recorded at the monomer mass channel under water-free conditions are shown in Figures 2−6. In all bands, a well-pronounced rotational structure covering a range from 3 to 5 cm^{-1} is resolved. The rotational structure of the bands at +42, +136, and +213 cm^{-1} is similar to the that of the published 0_0^0 band.[19] It is characterized by a central dip, a small Q branch on the red side of the dip, and well-defined P and R branches. The spectra of these

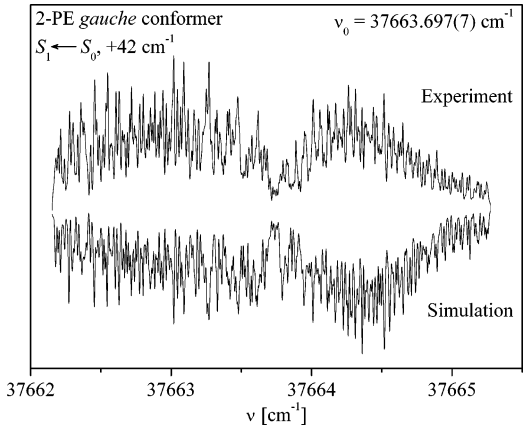

Figure 2. High-resolution two-color UV R2PI spectrum of vibronic band +42 cm^{-1} in Figure 1, recorded at m/z = 122. The band is assigned as a progression of the gauche conformer **2** of the 2-PE monomer with its rotationless transition centered at 37 663.697(7) cm^{-1}. Upper trace: experimental spectrum. Lower inverted trace: the best-fit simulated spectrum yielding the parameters in Table 1 (for details, see text).

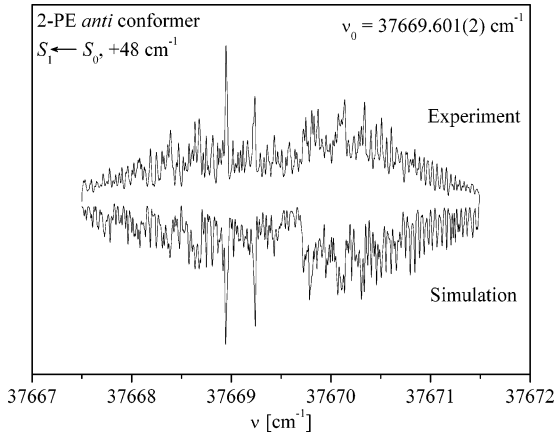

Figure 3. High-resolution two-color UV R2PI spectrum of vibronic band +48 cm^{-1} in Figure 1, recorded at m/z = 122. The band is assigned as a vibrational progression of the anti conformer **5** of the 2-PE monomer with the rotationless transition centered at 37 669.601-(2) cm^{-1}. Upper trace: experimental spectrum. Lower inverted trace: the best-fit simulated spectrum yielding the parameters in Table 1 (for details, see text).

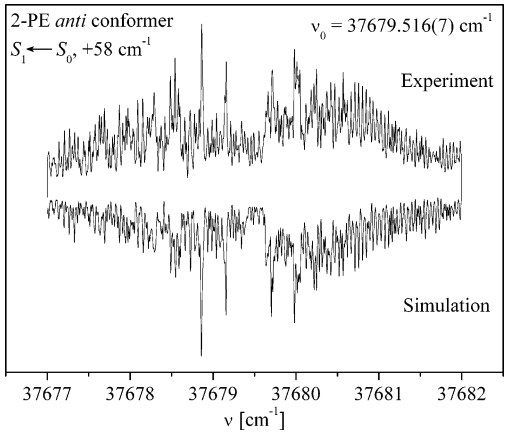

Figure 4. High-resolution two-color UV R2PI spectrum of vibronic band +58 cm^{-1} in Figure 1, recorded at m/z = 122. The band is assigned as a tunneling splitting of the anti conformer **5** of the 2-PE monomer with its rotationless transition centered at 37 679.516(7) cm^{-1}. Upper trace: experimental spectrum. Lower inverted trace: the best-fit simulated spectrum yielding the parameters in Table 1 (for details, see text).

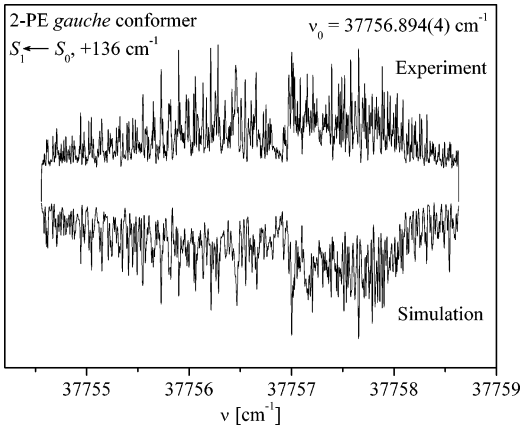

Figure 5. High-resolution two-color UV R2PI spectrum of vibronic band +136 cm^{-1} in Figure 1, recorded at m/z = 122. The band is assigned as a vibrational progression of the gauche conformer **2** of the 2-PE monomer with its rotationless transition centered at 37 756.894-(4) cm^{-1}. Upper trace: experimental spectrum. Lower inverted trace: the best-fit simulated spectrum yielding the parameters in Table 1 (for details, see text).

three bands manifest a hybrid *a*-, *b*-, and *c*-type character with prominent *b* contribution. They do not consist of single rotational lines but we observe peaks produced by aggregation of several rotational lines resulting in a minimum value for the peak width of 250 MHz fwhm. To find the rotational constants for the ground, S_0, and the first excited, S_1, electronic states, the transition moment ratio, the rotational temperature, and the origin position, ν_0, we used the computer-assisted rotational fit procedure based on genetic algorithm described earlier.[29−31] As starting values for our fits, we used the values resulting from ab inito calculations of the ground state rotational constants for the anti and gauche conformers. To minimize the number of simultaneously fitted parameters, we used a stepwise approach to determine the experimental values of all parameters. As a first step, we constrained the ground state rotational constants within 0.5% of their initial value and allowed the search space for the excited state rotational constants and for the other parameters to be relatively broad. In a second step, we used the values obtained in the first step and fixed the transition moment ratios but let the other parameters be free. The produced theoretical stick spectrum was convoluted using a Gaussian line shape with a fwhm of 150 MHz. The best-fit results for the bands are shown in the inverted spectra in Figures 2−6. The simulated spectra (the lower inverted part) agree well in both peak positions and peak intensities with the experimental ones (upper trace). The achieved cross correlation between the experimental and simulated spectra is as high as 95%. The experimentally obtained values of the rotational constants, the transition moment ratios, and the rotational temperatures are summarized in Table 1. Comparing the experimental values for the rotational constants with the results from the ab initio calculations, we can clearly assign the bands at +42, +136, and +213 cm^{-1} to the most stable gauche structure. However, differences are observed for the measured transition moment ratio of the + 42 cm^{-1} band from the +136 and +213 cm^{-1} bands and from theory. The experimental values for the +136 and +213 cm^{-1} bands (18:74:8) are the same as the ones of the 0_0^0 band[19] but differ from the theoretically predicted one at the MP2/cc-pVDZ level of theory (1:96:3). The measured mixed *a*- and *b*-type spectrum with transition moment ratio (42:50:8) of the +42 cm^{-1} band yields a transition moment orientation which is not predominantly along the *b* principal axis of inertia

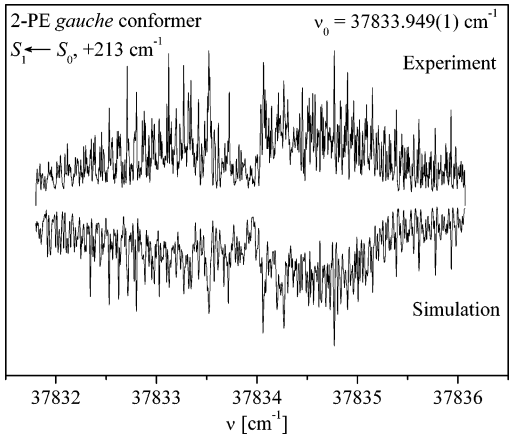

Figure 6. High-resolution two-color UV R2PI spectrum of vibronic band +213 cm^{-1} in Figure 1, recorded at m/z = 122. The band is assigned as a vibrational progression of the gauche conformer **2** of the 2-PE monomer with its rotationless transition centered at 37 833.949 cm^{-1}. Upper trace: experimental spectrum. Lower inverted trace: the best-fit simulated spectrum yielding the parameters in Table 1 (for details, see text).

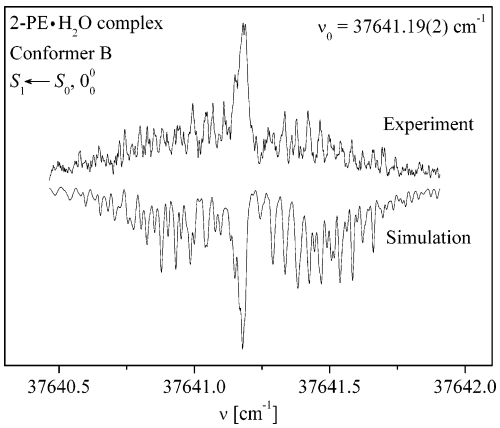

Figure 7. High-resolution two-color UV R2PI spectrum of band $1w_1$ in Figure 1, recorded at m/z = 140. The band is assigned as the 0_0^0 origin band of conformer **B** of the 2-PE•H_2O complex with the rotationless transition centered at 37 641.19(2) cm^{-1}. Upper trace: experimental spectrum. Lower inverted trace: the best-fit simulated spectrum yielding the parameters in Table 1 (for details, see text).

as is theoretically expected. On the other hand, the experimental rotational constants for both ground state and excited state are close to the ones of conformer **2**.

We used the above-described procedure to assign the spectra of the +48 and +58 cm^{-1} vibronic bands in Figures 3 and 4, fitting with a differing rotational band structure characterized by a minor central dip, a very small Q branch on the red side of the dip, and well-resolved P and R branches. Again, there is a good match in peak positions and peak intensities of measured and simulated spectra with achieved cross correlations of 96% and 95%, respectively. There is a good agreement between the values of rotational constants *B* and *C* in Table 1 and those found by our ab initio calculations of the anti conformer **5** for the ground, S_0, and the first excited, S_1, electronic states (cf. Table 3). Only the experimental and calculated values for the ground rotational constant *A* are somewhat different. In addition, the experimental values for the transition moment ratios of the two bands (4:96:0 and 8:92:0, respectively) are very close to the one calculated (0:100:0) for conformer **5**.

2. Water Complex Bands. Two of the vibrational bands, $1w_1$ and $3w_1$, measured at the parent mass channel (m/z = 140) of the singly hydrated complex of 2-PE (see Figure 1) have also been measured under high resolution. The low intensity of band $2w_1$ did not allow this band to be rotationally resolved. Band $3w_1$ yields relatively high intensity when measured by two-photon two-color ionization and spans a fairly broad (ca. 4 cm^{-1}) range. The band is superimposed on a high background, and its overall profile is characterized by two pronounced P and R branches and a shallow central dip with a weak Q branch. It is worth pointing out that the high intensity band $3w_1$ does not feature a resolved rotational microstructure. This precluded its rotational fit analysis.

The experimental highly resolved spectrum of band $1w_1$ is presented in Figure 7 (upper trace). The spectrum covers a relatively narrow frequency range of ca. 1.5 cm^{-1}. It has a well-resolved structure built up of separate peaks with a line width of 250 MHz resulting from aggregations of closely spaced single rotational lines. The spectrum lies on a small background, and features a prominent Q branch in the center and less intense P and R branches with irregular but resolved structures. We fitted the spectrum by the computer-aided routine based on genetic algorithms outlined above and derived the molecular parameters of the species producing it. The simulated stick spectrum was convoluted by a Gaussian profile with a line width of 150 MHz. The resulting best-fit simulated spectrum is depicted in Figure 7 (lower inverted trace). The simulation reproduces fairly well both the overall profile and peak positions. The so-obtained rotational constants for the ground, S_0, and the first excited, S_1, states, the transition moment ratio, the band origin position, ν_0, and the rotational temperature, *T*, are summarized in Table 2.

C. Ab Initio Calculations. Ab initio quantum chemistry calculations for various conformations of the 2-PE monomer and its singly hydrated complex have been performed using the Gaussian 03 program package.[32] Five different conformations of the 2-PE monomer and six different conformational structures of the 2-PE•H_2O complex have been considered.

1. 2-PE Monomer. To find the stable conformations of the 2-PE monomer, we performed a potential-energy grid search at the MP2/cc-pVDZ level of theory. The grid search was realized by scanning the C2C7C8O9 and C7C8O9H19 dihedral angles of the 2-PE molecule. The so-obtained potential energy surface is depicted in Figure 8 (for the sake of clear visualization the potential energy surface is inverted). Five potential energy minima have been predicted. The deepest one (global minimum) corresponds to the gauche conformer (conformer **2**), in which the terminal OH group of the side chain points to the π electrons of the aromatic ring. Two other higher energy structures (conformer **1** and conformer **3**) separated from each other, and from the main minimum, by low potential barriers correspond also to gauche conformations but with different orientations of the OH group (different C7C8O9H19 dihedral angles). The conformations with the side chain pointing away from the benzene ring (conformer **4** and conformer **5**) are referred to as anti conformers, and they give rise to the other two potential energy minima. The two structures in question are separated by a low potential barrier from each other, and by a high barrier along the C2C7C8O9 angle coordinate from the gauche conformers. The conformational structures corresponding to the potential energy minima have been subjected to a further full structural optimization and calculation of their energetics at the MP2/cc-pVDZ level of theory for the ground, S_0, electronic state, and at the CIS/cc-pVDZ level of theory for the first excited, S_1, electronic state. In addition, a frequency analysis for both ground, S_0, and first excited, S_1, electronic states has been performed at the same level of theory, respectively. The presence of only positive frequencies is a verification that the

TABLE 1: Experimental Rotational Constants for the Ground, S_0 (A'', B'', C''), and the First Excited, S_1 (A', B', C'), Electronic States, the Transition Moment Ratio, μ_a^2:μ_b^2:μ_c^2, the Band Origin Frequency, ν_0, the Rotational Temperature, T, and the Best-Fit Cross Correlation Obtained from the Rotational Fit of Bands +42, +48, +58, +136, and +213 cm^{-1} Shown in Figures 1−6[a]

	band				
parameter	+42 cm^{-1}	+48 cm^{-1}	+58 cm^{-1}	+136 cm^{-1}	+213 cm^{-1}
A'', cm^{-1}	0.111 6(11)	0.147 65(19)	0.147 85(30)	0.111 3(22)	0.111 8(25)
B'', cm^{-1}	0.036 05(32)	0.028 41(9)	0.028 57(34)	0.036 20(63)	0.036 11(63)
C'', cm^{-1}	0.032 11(28)	0.025 57(8)	0.025 58(41)	0.032 03(35)	0.031 92(33)
A', cm^{-1}	0.108 3(14)	0.141 18(14)	0.141 22(27)	0.108 0(32)	0.108 6(26)
B', cm^{-1}	0.035 38(33)	0.028 03(7)	0.028 18(39)	0.035 60(49)	0.035 50(56)
C', cm^{-1}	0.031 28(45)	0.025 13(9)	0.025 13(42)	0.031 10(47)	0.031 09(34)
μ_a^2:μ_b^2:μ_c^2	42:50:8	8:92:0	4:96:0	19:74:9	19:74:9
ν_0 (cm^{-1})	37 663.697(7)	37 669.601(2)	37 679.516(7)	37 756.894(4)	37 833.949(1)
T (K)	8.5(2)	8.6(3)	9.9(2)	11.3(5)	11.2 (1)
best-fit cross correlation (%)	94.5	95.6	95.2	94.7	95.6

[a] The numbers in parentheses represent one standard deviation in units of the least significant quoted digit. The uncertainty for the relative values μ_a^2, μ_b^2, and μ_c^2 in the transition moment ratio does not exceed 5%.

TABLE 2: Experimental Rotational Constants for the Ground, S_0 (A'', B'', C''), and the First Excited, S_1 (A', B', C'), Electronic States, the Transition Moment Ratio, μ_a^2:μ_b^2:μ_c^2, the Band Origin Frequency, ν_0, the Rotational Temperature, T, and the Best-Fit Cross Correlation Obtained from Rotational Fit of the 0_0^0 Origin Band of the $S_1 \leftarrow S_0$ Electronic Transition of Conformer B of the 2-PE·H_2O Complex Shown in Figure 7[a]

parameter	band: $1w_1$
A'', cm^{-1}	0.0671(9)
B'', cm^{-1}	0.0270(3)
C'', cm^{-1}	0.0224(10)
A', cm^{-1}	0.0654(14)
B', cm^{-1}	0.0268(3)
C', cm^{-1}	0.0221(1)
μ_a^2:μ_b^2:μ_c^2	69:31:0
ν_0 (cm^{-1})	37 641.19(2)
T (K)	1.4(1)
best-fit cross correlation (%)	91

[a] The numbers in parentheses represent one standard deviation in units of the least significant quoted digit. The uncertainty for the relative values μ_a^2, μ_b^2, and μ_c^2 in the transition moment ratio is 9%.

optimized structures indeed correspond to potential energy minima. The rotational constants of the discussed conformations for both ground and excited electronic states along with the energies without and with the zero-point vibrational energy (ZPVE) corrections for the ground state, and the transition moment ratios for the first excited electronic state, as well as some typical interatomic distances, planar angles, and dihedral angles are summarized in Table 3. The fully optimized conformations are also shown in Figure 8 atop their corresponding points on the potential energy surface. The vibrational frequencies for the first excited, S_1, electronic state are detailed in Table 4. In addition to the above-described calculations, structural optimizations and energy calculations of conformers **4** and **5** at the MP2/aug-cc-pVTZ level of theory have been performed as well. The use of this very extended basis set significantly accounting for the electron correlation was expected to resolve the existing controversy[3,7,15] on the energy ordering of conformer **4** and conformer **5**, and to theoretically substantiate our experimental results. No noticeable structural changes occur upon extending the basis set from cc-pVDZ to aug-cc-pVTZ, but at the augmented basis set conformer **5** is more stable than conformer **4** by 53 cm^{-1}. This result does not include the ZPVE since the vibrational analysis of the two conformations at this basis set is computationally very expensive. The inclusion of the ZPVE, however, is not expected to alter the relative energy ordering of the two conformers.

2. 2-PE·H_2O Complex. As an initial step, we performed structural optimizations for the ground, S_0, and the first excited, S_1, electronic states at the MP2/6-31G* and CIS/6-31G* levels of theory, respectively, of various conformations of the 2-PE·H_2O complex. The starting geometries of the hydrated complexes were conceived by attaching the water moiety to different plausible binding sites of the three lowest-energy conformations (conformers **2**, **4**, and **1**) of the 2-PE monomer. In this way, six different conformations of the 2-PE·H_2O complex were produced and optimized (Figure 9). The theoretically predicted inertial parameters for the ground and excited states and the transition moment ratio were used to simulate theoretical spectra, which were visually compared with the experimental highly resolved spectrum of the 2-PE·H_2O complex (see Figure 7, upper trace). The apparent disagreement between the experimental spectrum and the simulated spectra corresponding to the two hydrated complexes when involving the anti conformer of the 2-PE monomer (conformer **4**) was a clear indication that the experimental spectrum does not originate from either of these two complexes. For this reason the latter were ruled out from further consideration. The remaining four structures of the 2-PE·H_2O complex were subjected to further full geometrical optimizations and vibrational analysis for both ground, S_0, and first excited, S_1, electronic states at the MP2/cc-pVDZ and CIS/cc-pVDZ levels of theory, respectively, thus improving the electron correlation. In this way various binding patterns have been thoroughly theoretically explored, in which water plays the role of either a proton donor or a proton acceptor forming σ or π weak intermolecular hydrogen bonds. The found vibrational frequencies of all optimized conformers are positive, which is a verification that indeed those structures correspond to minima on the potential energy surface. We also calculated the binding energies without and including the basis set superposition error (BSSE) and zero-point vibrational energy (ZPVE). The absolute binding energies depend essentially on the inclusion of the corrections accounting for the BSSE and ZPVE, but the energy ordering of the conformations remains always the same. The rotational constants for both the ground state and the first excited electronic state, binding energies for the ground state, and the transition electronic dipole moments of all conformations are summarized in Table 5. The optimized conformational shapes are depicted in Figure 9, where conformers **A**, **B**, **C**, and **D** have been optimized at the MP2/cc-pVDZ level of theory, and conformers **E** and **F** (presented for completeness) have been optimized at the MP2/6-31G* level of theory. The most stable conformer (the one with the highest binding energy) is conformer **A**, in which the water molecule

TABLE 3: Theoretical Interatomic Distances, *d*, Planar Angles, α, Dihedral Angles, *τ*, and Rotational Constants, *A*, *B*, and *C*, for the Ground, S_0, and the First Excited, S_1, Electronic States of the gauche and anti Conformers of the 2-PE Monomer Calculated at the MP2/cc-pVDZ and CIS/cc-pVDZ Levels of Theory, Respectively[a]

	gauche						anti			
	conformer **1**		conformer **2**		conformer **3**		conformer **4**		conformer **5**	
	S_0	S_1	S_0	S_1	S_0	S_1	S_0	S_1	S_0	S_1
d(H15−C1), Å	3.78	3.89	2.54	2.78	3.41	3.53				
α_1(C1C2C7), deg	120.8	120.9	120.5	120.6	121.1	122.1	120.5	120.4	120.7	120.6
α_2(C2C7C8), deg	112.7	114.7	110.8	113.8	113.3	116.8	111.2	113.3	111.0	113.1
α_3(C7C8O9), deg	107.7	108.9	112.3	113.0	113.1	114.1	112.8	112.0	107.5	107.5
α_4(C8O9H15), deg	106.9	109.5	105.6	109.0	105.9	109.2	106.1	109.3	106.7	109.4
τ_1(C3C2C7C8), deg	10.4	105.1	90.0	90.6	109.9	140.8	89.4	90.3	88.5	89.3
τ_2(C2C7C8O9), deg	69.3	70.6	60.5	64.8	67.4	71.6	176.7	177.3	0	0
τ_3(C7C8O9H19), deg	−168.6	−170.7	−61.6	65.3	66.5	63.1	−63.3	−67.0	0	0
A, cm^{-1}	0.116 22	0.117 16	0.110 23	0.112 00	0.117 07	0.125 53	0.144 49	0.144 57	0.145 70	0.145 42
B, cm^{-1}	0.035 77	0.034 81	0.036 77	0.035 24	0.035 26	0.033 74	0.028 31	0.028 12	0.02840	0.028 19
C, cm^{-1}	0.029 75	0.029 09	0.031 76	0.030 47	0.02921	0.027 40	0.025 33	0.025 08	0.025 41	0.025 16
$\mu_a^2:\mu_b^2:\mu_c^2$		18:77:5		1:96:3		23:77:0		0:100:0		0:100:0
E_{rel}, cm^{-1}	652.78		0		703.59		649.69		769.00	
E_{rel}(incl ZPVE), cm^{-1}	685.86		0		783.30		586.00		788.35	

[a] Electric dipole transition moment (TM) ratio, $\mu_a^2:\mu_b^2:\mu_c^2$, were obtained from CIS/cc-pVDZ calculation of the optimized geometry of the 2-PE monomer. Relative energies, E_{rel}, of the five most stable conformational structures of the 2-PE monomer without and with inclusion of the zero-point vibrational energy were calculated at the MP2/cc-pVDZ level of theory.

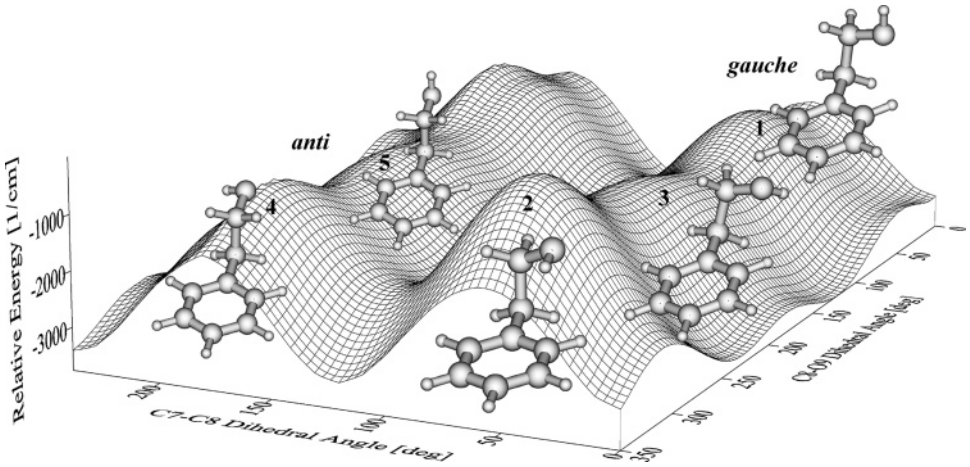

Figure 8. Potential energy surface (inverted for the sake of a better visualization) as a function of the C2C7C8O9 and C7C8O9H19 dihedral angles of the 2-PE monomer. The gauche and anti conformations are separated by a high potential barrier in the C7C8 coordinate. The five energetically most favorable conformations of the 2-PE monomer have been fully geometrically optimized in their ground, S_0, electronic state at the MP2/cc-pVDZ level of theory. The fully optimized structures are depicted on their corresponding minima on the potential energy surface.

TABLE 4: Theoretical Lowest Vibrational Frequencies for the First Excited, S_1, Electronic State of the gauche and anti Conformations of the 2-PE Monomer, Calculated at the CIS/cc-pVDZ Level of Theory[a]

conformer **1**		conformer **2**		conformer **3**		conformer **4**		conformer **5**	
ν, cm^{-1}	mode	*ν*, cm^{-1}	mode	*ν*, cm^{-1}	mode	*ν*, cm^{-1}	mode	*ν*, cm^{-1}	mode
31	torsion	45	torsion	26	torsion	42	torsion	40	torsion
102	stretching	89	stretching	120	bending	88	bending	89	bending
129	torsion	135	torsion	148	torsion	99	torsion	96	torsion
226	bending	230	stretching	232	bending	230	bending	232	bending

[a] The applied scale factor is 0.94.

inserts between the benzene ring and the side chain of the most stable 2-PE monomer (conformer **2**). In this bridging structure the water molecule acts as both a proton donor and a proton acceptor, forming a weak π hydrogen bond with the benzene ring and a σ bond with the hydrogen atom of the terminal hydroxyl group of 2-PE. The second-in-energy conformer is conformer **B**, in which the water moiety binds sideways to 2-PE through the formation of a single σ bond wherein the water molecule donates a proton to the oxygen atom of the OH group of 2-PE. The higher energy conformers of the 2-PE·H_2O complex involve conformer **1** of the 2-PE monomer.

IV. Discussion

A. Monomer Conformers. In our ab inito calculations of the 2-PE monomer at the MP2/cc-pVDZ level of theory, we have considered five of the most stable 2-PE monomer structures which have been discussed in previous works.[5,14,15,17,18] The most stable conformer is the one with the hydroxyl hydrogen positioned above the benzene ring, and designated hereinafter as conformer **2**. The next two conformations are the anti conformer **4** and the gauche conformer **1**, separated from the most stable species by 586 and 685.86 cm^{-1}, respectively. The energy gap between them, however, is very small, and therefore

TABLE 5: Theoretical Interatomic Distances, *d*, Planar Angles, α, Dihedral Angles, *τ*, and Rotational Constants, *A*, *B*, and *C*, for the Ground, S_0, and the First Excited, S_1, Electronic States of the Singly Hydrated Complexes of 2-PE Calculated at the MP2/cc-pVDZ and CIS/cc-pVDZ Levels of Theory, Respectively[a]

	conformer **A** (conformer **2**)		conformer **B** (conformer **2**)		conformer **C** (conformer **1**)		conformer **D** (conformer **1**)	
conformer	S_0	S_1	S_0	S_1	S_0	S_1	S_0	S_1
d(H15−C1), Å	2.93	3.17	2.52	2.86	4.02	4.19	3.95	4.11
α_1(C1C2C7), deg	120.4	120.5	120.2	120.4	120.4	120.7	120.6	120.7
α_2(C2C7C8), deg	111.0	114.1	110.6	113.6	112.1	114.4	112.0	114.4
α_3(C7C8O9), deg	112.1	112.9	112.1	112.9	107.9	104.2	107.4	108.8
α_4(C8O9H15), deg	105.8	109.3	105.3	108.9	107.2	109.6	106.5	109.2
τ_1(C3C2C7C8), deg	88.7	84.3	87.5	85.2	88.8	82.9	93.2	90.9
τ_2(C2C7C8O9), deg	58.9	63.7	58.3	63.2	63.6	67.0	63.8	66.0
τ_3(C7C8O9H19), deg	−88.2	−87.0	−57.7	−65.5	−177.8	−172.9	176.9	177.0
d(O9−H21), Å	1.87	2.01	1.91	2.05	1.89	2.02	2.04	2.18
α_5, deg	101.9	109.4	162.5	159.3	167.3	170.8	150.6	146.2
τ_4, deg	−0.6	−26.8	62.9	61.3	−160.2	174.3	67.0	59.1
A, cm^{-1}	0.063 83	0.060 38	0.067 48	0.064 38	0.066 73	0.061 98	0.064 37	0.059 07
B, cm^{-1}	0.032 72	0.031 18	0.027 63	0.026 60	0.026 91	0.026 66	0.031 20	0.029 92
C, cm^{-1}	0.028 98	0.027 17	0.022 56	0.021 25	0.021 81	0.020 77	0.028 70	0.026 53
TM ratio, μ_a^2:μ_b^2:μ_c^2		24:1:75		71:29:0		85:10:5		14:2:84
E_{rel}, cm^{-1}	0		216		463		391	
E_{rel}(BSSE), cm^{-1}	0		460		725		628	
E_{rel}(BSSE + ZPVE), cm^{-1}	0		94		240		131	

[a] α_5 denotes angle H19O20H22 in conformer **A** and angle O9H21O20 in conformers **B**, **C**, and **D**, respectively. τ_4 designates dihedral angle O9H19O20H22 in conformer **A** and dihedral angle H19O9H21O20 in conformers **B**, **C**, and **D**, respectively. Electric dipole transition moment (TM) ratio, μ_a^2:μ_b^2:μ_c^2, was obtained from CIS/cc-pVDZ calculation of the optimized geometry of the 2-PE·H_2O complex. Relative energies, E_{rel}, of the four most stable conformational structures of the singly hydrated complex of 2-PE without and with inclusion of the basis set superposition error (BSSE) correction and zero-point vibrational energy were obtained from MP2/cc-pVDZ calculations. The parent conformations of 2-PE giving rise to the respective hydrated complexes are reported in parentheses in the header of the table. For details, see text.

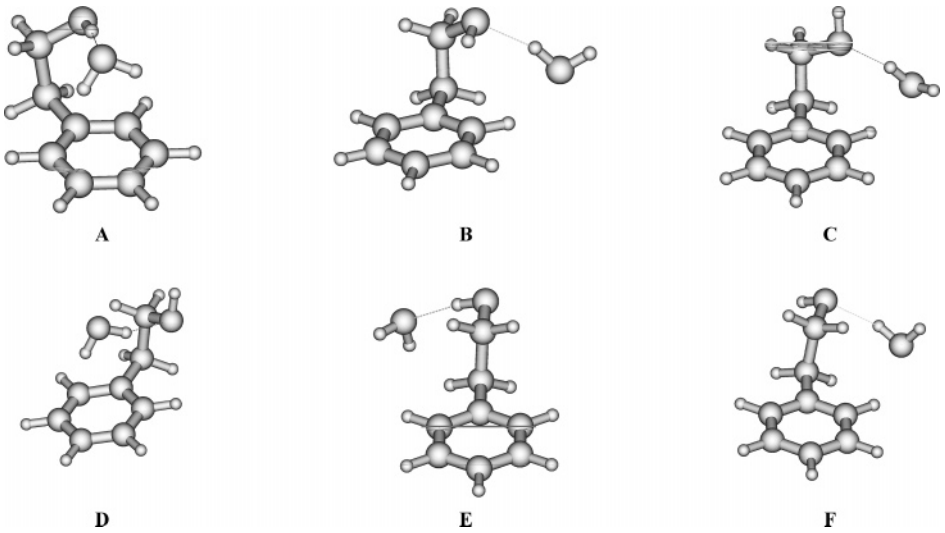

Figure 9. Electronic ground state, S_0, structures of the 2-PE·H_2O complex optimized at the MP2/cc-pVDZ (conformers **A**, **B**, **C**, and **D**) and MP2/6-31G* level of theory, respectively. Typical angles, bond lengths, inertial parameters, and binding energies for these structures are listed in Table 5.

the above ordering may be changed upon improving the used computational method and basis set. The most unstable conformations are the gauche conformer **3**, and the anti conformer **5**, distanced by 783.30 and 788.35 cm^{-1} from the lowest-energy conformer **2**. We unambiguously assign bands +136 and +213 cm^{-1} to conformer **2**, where the agreement of the theoretical and experimental values for the rotational constants of the ground, S_0, and the first excited, S_1, electronic states and the transition moment ratio is the best. This is the conformer that produces also the strongest band (see Figure 1).[19] In the case of band +42 cm^{-1}, where the transition moment ratio differs form the one predicted for conformer **2**, the assignment is based on the rotational constants' match only. A similar to our (42:50:8) change of the transition moment ratio has been predicted (42:36:22) by Mons et al.[14] We support their explanation for the origin of this phenomenon: the +42 cm^{-1} band may gain intensity through vibronic coupling to another excited electronic state, which leads to a strong dependency of the transition moment ratio on the nature of the vibration.

An additional argument that conformer **2** produces the bands at +42, +136, and +213 cm^{-1} is the good agreement between the band positions and the theoretically predicted fundamental vibrational frequencies for this conformer (see Table 4). On the basis of the above vibrational analysis, we tentatively conclude that the very weak band at +90 cm^{-1} also originates from conformer **2** of the 2-PE monomer. The other unassigned weak band at +75 cm^{-1} is very likely to stem from fragmentation of a water complex of 2-PE.

The calculated inertial parameters of conformers **4** and **5** are very similar with the exception of rotational constant *A*. This is not surprising, noting that these two structures differ from each other only by the orientation of the terminal OH group of the

side chain. Notwithstanding the similarity of the theoretically predicted rotational constants of the discussed conformers, the rotational fit of our high-resolution spectra unambiguously demonstrates that both vibrational bands at +48 and +58 cm^{-1} originate from structure **5**. This assignment is in agreement with the finding of Mons et al.[14] based on UV−UV hole burning and infrared spectroscopy. The assignment of band +48 cm^{-1} as originating from conformer **5** is corroborated also by dispersed fluorescence experiments.[18] Both close-lying bands with similar rotational structures, +48 and +58 cm^{-1}, may result from transitions from conformer **5** in the electronic ground, S_0, state to conformers **4** and **5** in the first excited, S_1, electronic state due to the torsional potential for the hydroxyl hydrogen in the electronically excited state favoring these transitions.[14] This is a plausible explanation since, in the anti conformers **4** and **5**, the behavior of the OH group is almost negligibly perturbed by the rest of the molecule and, for this reason, its properties are expected to bear a resemblance to the ones of the OH group in ethanol. Hence the OH potential energy model for ethanol[33] can be applied to the *anti*-2-phenylethanol as well. A like phenomenon has been observed also for *p*-tyrosol.[34]

All vibrational bands measured under high resolution have been successfully assigned to conformers **2** and **5**, respectively. No evidence for the existence of the other three conformers has been found. This puts forward the following issues: (i) why only two out of five theoretically predicted conformational structures have been experimentally observed; (ii) why the highest-energy conformer **5** is observed in the cold molecular beam rather than any of the low-lying structures. The explanation of the first question requires cognizance of the potential energy surface and discussion of the relaxation dynamics during the process of the adiabatic expansion, presuming that in the preexpansion region of the nozzle there exist several different conformational structures at room temperature that relax during the process of the adiabatic cooling. As seen from the shape of the potential energy surface depicted in Figure 8, the gauche conformers are separated from the anti conformers by a high potential barrier, whereas the potential barriers between the gauche conformers and between the anti conformers, respectively, are very low. Therefore, we may conclude that the high potential barrier precludes the interconversion between gauche and anti conformers on one hand, and on the other hand the low potential barriers between the gauche and anti conformers, respectively, favor the relaxational intraconversion within the two groups of species during the expansion. Thus, it is plausible to assume that under such circumstances the gauche conformers relax to the most stable gauche conformer, which is the most stable conformer as well, and the anti conformers relax to the lowest-energy anti conformer. It is not clear, however, why the experimentally observed anti conformer is conformer **5**, which is less stable by 202.35 cm^{-1} than conformer **4** as predicted at the MP2/cc-pVDZ level of theory. Experimental evidence for the existence of conformer **5** has been presented also by microwave spectroscopy.[15] To clarify this question, we performed additional ab initio quantum chemistry calculations with a very extended basis set for these two conformers. Augmenting the basis set, we have found that at the MP2/aug-cc-pVTZ level of theory with an improved electron correlation conformer **5** is energetically more stable than conformer **4** by 45 cm^{-1}. This fact combined with the presumed low potential barrier between the two conformers also at the MP2/aug-cc-pVTZ level of theory favors a fast and efficient relaxation of conformer **4** to conformer **5**, and, hence, the experimental observation of the latter.

B. 2-PE·H_2O Conformer. Comparing the rotational constants for the ground, S_0, and the first excited, S_1, electronic states and the transition moment ratio obtained from the fit of the highly resolved two-photon two-color spectrum measured at the parent ($m/z = 140$) channel of the singly hydrated complex of 2-PE with the respective theoretically predicted inertial parameters and transition moment ratios of the optimized structures of the complex, we have concluded that band $1w_1$ originates from the 2-PE·H_2O conformer **B**. In conformer **B** water binds sideways to the most stable (conformer **2**) conformer of 2-PE through the formation of a strong single σ hydrogen bond (bond length 1.9 Å), wherein water donates a proton to the oxygen atom of the side-chain hydroxyl group of 2-PE. The theoretically predicted distance between the O atom of the water moiety and the nearest hydrogen atom from the benzene ring is 2.44 Å, which is likely to suggest the existence of an additional weak σ hydrogen bond in which the water molecule is a proton acceptor. This assumption is somewhat justified by the well-resolved structure of this band, which is typical for rigid or almost rigid complexes where the position of the attached species is fixed and the relative motions of the two moieties are strongly constrained. Since the two hydrogen bonds are almost perpendicular to each other, the existence of the above-mentioned additional weak σ hydrogen bond is supposed to hinder the tumbling motion of the water moiety about the strong σ hydrogen bond, thus preventing complication of the rotational structure of the spectrum. The relatively small theoretically predicted energy gap of 94 cm^{-1} from the most stable conformer (conformer **A**) can also be attributed to the assumed additional hydrogen bond. Comparing the geometrical parameters (interatomic distances, planar angles, and dihedral angles) of the 2-PE molecule (conformer **2**) in the bare state (see Table 3) and in the complex with water (see Table 5), one can infer that no appreciable structural changes or deformations of the 2-PE species take place upon complexation with water. This demonstrates that the backbone of the host *gauche*-2-PE conformer is stabilized by an intramolecular hydrogen bond between the terminal OH group and the π electrons of the benzene ring, which is stronger than the intermolecular hydrogen bonds responsible for the water attachment. A conspicuous difference, however, is observed between the transition moment ratios of 2-PE monomer (conformer **2**) and its singly hydrated complex (conformer **B**). Since in the latter the π electrons of the aromatic chromophore are not involved in the interaction with the water moiety, it is very unlikely that there is an alteration of the transition moment vector relative to the benzene ring. We attribute the observed drastic change of the transition moment ratio as a pure mass effect descending from reorientation of the principal axes of inertia due to the attachment of a water molecule. It is important to note that, after excitation of band $1w_1$, the 2-PE·H_2O does not fragment under the water-in conditions of two-photon one-color experiments as no trace of a signal has been observed at the parent mass channel of the monomer ($m/z = 122$); this points to a stable complex.

An interesting issue is the search for the theoretically predicted most stable conformer of the 2-PE·H_2O complex (conformer **A**). Since conformer **A** is predicted to be the most stable one, this suggests that it must yield a high-intensity band. This is, however, not the case for band $2w_1$, and we tentatively assign band $3w_1$ as originating from conformer **A**. The high intensity of this band is in line with the above discussion. The unresolved rotational structure of this band can be explained by a tumbling motion of the intercalated water moiety about the π intermolecular hydrogen bond. Unlike the case of

conformer **B**, where the two intermolecular bonds are almost perpendicular, in this case, the two intermolecular bonds, the OH···π and the H−O σ bonds, lie almost on a straight line, and the rotation of the water molecule about the π hydrogen bond is not hindered, which leads to a broadening and smearing of the rotational structure of the spectrum. Our assignment is in line with the one of Hockridge et al.,[8] and we also observe fragmentation of band $3w_1$ into the mass channel of the 2-PE monomer ($m/z = 122$).

Hockridge et al.[8] have assigned band $2w_1$ to conformer **B**, and band $1w_1$ does not appear at the mass channel of the singly hydrated complex of 2-PE ($m/z = 122$). We have performed a one-color experiment monitoring the mass channel of the doubly hydrated complex of 2-PE, but we did not observe any peaks. It is very unlikely that on one hand the abundance of doubly hydrated complexes of 2-PE in the molecular beam is high, and on the other hand they fragment completely to singly hydrated complexes so as to yield an intensity commensurate to the intensity of the most stable conformer **A** (band $3w_1$).

V. Summary and Conclusions

2-PE, the hydroxy analogue of the simplest aromatic neurotransmitter, 2-phenylethylamine, and its singly hydrated complex have been investigated by a combination of mass selective high-resolution two-color R2PI spectroscopy and quantum chemistry ab initio calculations. All prominent blue-shifted vibronic bands of the 2-PE monomer up to 220 cm^{-1} have been measured at high resolution of 100 MHz. On the basis of comparison of the inertial parameters obtained from the analysis of the highly resolved spectra and those resulting from the structural optimizations of the lowest-energy conformations of 2-PE, we were able to assign all five bands as resulting from two conformers: the lowest-energy gauche conformer and the second-in-energy anti conformer of 2-PE. This structural assignment is corroborated by the fair agreement between the theoretically predicted vibrational frequencies for the gauche and anti conformers and the vibrational band positions. The observation of only two out of five theoretically predicted conformations under the conditions of molecular jet expansion in conjunction with a detailed theoretical study of the potential energy surface of 2-PE has put forward the issue of conformational interconversion. Our calculations demonstrate that the gauche conformers as well as the anti conformers are separated from one another by only low potential barriers, while the gauche and the anti conformers are separated by a significant potential barrier. On this basis we conclude that in the process of adiabatic jet expansion all gauche conformers relax to the most stable gauche conformer, which is also the lowest-energy conformer of 2-PE, and the anti conformers relax to the most stable anti conformer. The high potential energy barrier between them, however, precludes the anti conformers from a further relaxation to the most stable gauche geometry of conformer **2**. This corollary implies that energy considerations alone are not sufficient for an adequate explanation of the observed structures. It is important also that the relaxational kinetics in the expansion process be considered.

It is known that that the properties of many biologically relevant molecules depend substantially on their environment. To elucidate this issue, as a first step, we investigated the complexation of 2-PE with a single water molecule. Comparing the results from the high-resolution experiment with those from ab initio calculations, we have found that the most stable conformers of the singly hydrated complex of 2-PE belong to the most stable structure of the monomer. The relatively scarce vibronic spectrum of the 2-PE·H_2O complex (only three bands) implies that the many different conformations of the singly hydrated complex of 2-PE which are theoretically supposed to exist in the preexpansion region either dissociate or relax to two stable conformations presumably separated by a high potential barrier, which precludes the interconversion of the higher-lying conformer to the most stable one. We did not observe significant structural changes of the 2-PE monomer upon its complexation with a single water molecule within our experimental resolution, which is an indication that in the case of the gauche conformer of 2-PE, the intramolecular hydrogen bond still dominates over the intermolecular hydrogen bonds responsible for the water attachment. From this we can conclude that a more complete solvation shell is necessary to bring about structural changes of the host molecule, and a systematic investigation of the influence of increasing the number of solvent molecules on the structure of flexible biologically relevant species is intended.

Acknowledgment. Financial support from the Deutsche Forschungsgemeinschaft and the Fonds der Chemischen Industrie is gratefully acknowledged.

References and Notes

(1) Zigmond, M. F. *Fundamental Neuroscience*; Academic Press: London, 1998.
(2) Snyder, S. H. *Drugs and the Brain*; Scientific American Library: New York, 1999.
(3) Godfrey, P. D.; Brown, R. D.; Hatherley, L. D. *J. Am. Chem. Soc.* **1995**, *117*, 8204.
(4) Sun, S.; Bernstein, E. R. *J. Am. Chem. Soc.* **1996**, *118*, 5086.
(5) Dickinson, J. A.; Hockridge, M. R.; Kroemer, R. T.; Robertson, E. G.; Simons, J. P.; McCombie, J.; Walker, M. *J. Am. Chem. Soc.* **1998**, *120*, 2622.
(6) Martinez, S. J., III; Alfano, J. C.; Levy, D. H. *J. Mol. Spectrosc.* **1998**, *158*, 82.
(7) Guchhait, N.; Ebata, T.; Mikami, N. *J. Am. Chem. Soc.* **1999**, *121*, 5705.
(8) Hockridge, M.; Robertson, E. G. *J. Phys. Chem. A* **1999**, *103*, 3618.
(9) Lee, Y.; Jung, J.; Kim, B.; Butz, P.; Snoek, L. C.; Kroemer, R. T.; Simons, J. P. *J. Phys. Chem. A* **2004**, *108*, 69.
(10) Butz, P.; Macleod, N. A.; Snoek, L. C.; Talbot, F. O.; Simons, J. P. *Central Laser Facility Annual Report 2000/2001*; Oxford University: Oxford, UK, 2002; p 97.
(11) Butz, P.; Kroemer, R. T.; Macleod, N. A.; Simons, J. P. *J. Phys. Chem. A* **2001**, *105*, 544.
(12) Karaminkov, R.; Chervenkov, S.; Härter, P.; Neusser, H. J. *Chem. Phys. Lett.* **2007**, *442*, 238.
(13) Butz, P.; Kroemer, R. T.; Macleod, N. A.; Robertson, E. G.; Simons, J. P. *J. Phys. Chem. A* **2001**, *105*, 1050.
(14) Mons, M.; Robertson, E. G.; Snoek, L. C.; Simons, J. P. *Chem. Phys. Lett.* **1999**, *310*, 423.
(15) Godfrey, P. D.; Jorissen, R. N.; Brown, R. D. *J. Phys. Chem. A* **1999**, *103*, 7621.
(16) Weinkauf, R.; Lehrer, F.; Schlag, E. W.; Metsala, A. *Faraday Discuss.* **2000**, *115*, 363.
(17) Brown, R. D.; Godfrey, P. D. *J. Phys. Chem. A* **2000**, *104*, 5742.
(18) Panja, S. S.; Chakraborty, T. *J. Phys. Chem. A* **2003**, *107*, 10984.
(19) Chervenkov, S.; Karaminkov, R.; Braun, J. E.; Neusser, H. J.; Panja, S. S.; Chakraborty, T. *J. Chem. Phys.* **2006**, *124*, 234302.
(20) Zwier, T. S. *J. Phys. Chem. A* **2001**, *105*, 8827.
(21) Borst, D. R.; Joireman, P. W.; Pratt, D. W.; Robertson, E. G.; Simons, J. P. *J. Chem. Phys.* **2002**, *116*, 7057.
(22) Florio, G. M.; Zwier, T. S. *J. Phys. Chem. A* **2003**, *107*, 974.
(23) Schmitt, M.; Böhm, M.; Ratzer, C.; Vu, C.; Kalkman, I.; Meerts, W. L. *J. Am. Chem. Soc.* **2005**, *127*, 10356.
(24) Nguyen, T. V.; Yi, J. T.; Pratt, D. W. *Phys. Chem. Chem. Phys.* **2006**, *8*, 1049.
(25) Alvarez-Valtierra, L.; Pratt, D. W. *J. Chem. Phys.* **2007**, *126*, 224308.
(26) Sussmann, R.; Neuhauser, R.; Neusser, H. J. *Can. J. Phys.* **1994**, *72*, 1179.
(27) Neusser, H. J.; Siglow, K. *Chem. Rev.* **2000**, *100*, 3921.
(28) Chervenkov, S.; Wang, P. Q.; Karaminkov, R.; Chakraborty, T.; Braun, J. E.; Neusser, H. J. *Proc. SPIE* **2005**, *5830*, 246.

(29) Chervenkov, S.; Wang, P. Q.; Braun, J. E.; Neusser, H. J. *J. Chem. Phys.* **2004**, *121*, 7169.

(30) Chervenkov, S.; Wang, P. Q.; Braun, J. E.; Georgiev, S.; Nandi, C. K.; Chakraborty, T.; Neusser, H. J. *J. Chem. Phys.* **2005**, *122*, 244312.

(31) Chervenkov, S.; Wang, P.; Braun, J. E.; Chakraborty, T.; Neusser, H. J. *Phys. Chem. Chem. Phys.* **2007**, *9*, 837.

(32) Frisch, M. J.; Trucks, G. W.; Schlegel, H. B.; Scuseria, G. E.; Robb, M. A.; Cheeseman, J. R.; Montgomery, J. A., Jr.; Vreven, T.; Kudin, K. N.; Burant, J. C.; Millam, J. M.; Iyengar, S. S.; Tomasi, J.; Barone, V.; Mennucci, B.; Cossi, M.; Scalmani, G.; Rega, N.; Petersson, G. A.; Nakatsuji, H.; Haga, M.; Ehara, M.; Toyota, K.; Fukuda, R.; Hasegawa, J.; Ishida, M.; Nakajima, T.; Honda, Y.; Kitao, O.; Nakai, H.; Klene, M.; Li, X.; Knox, J. E.; Hratchian, H. P.; Cross, J. B.; Adamo, C.; Jaramillo, J.; Comperts, R.; Stratmann, R. E.; Yazyev, O.; Austin, A. J.; Cammi, R.; Pomelli, C.; Ochterski, J. W.; Ayala, P. Y.; Morokuma, K.; Voth, J. A.; Salvador, P.; Dannenberg, J. J.; Zakrzewski, V. G.; Dapprich, S.; Daniels, A. D.; Strain, M. C.; Farkas, O.; Malick, D. K.; Rabuck, A. D.; Raghavachari, K.; Foresman, J. B.; Ortiz, J. V.; Cui, Q.; Baboul, A. G.; Clifford, S.; Cioslowski, J.; Stefanov, B. B.; Liu, G.; Liashenko, A.; Piskorz, P.; Kamaromi, I.; Martin, R. L.; Fox, D. J.; Keith, T.; Al-Laham, M. A.; Peng, C. Y.; Nanayakkara, A.; Challacombe, M.; Gill, P. M. W.; Johnson, B.; Chen, W.; Wong, M. W.; Gonzales, C.; Pople, J. A. *Gaussian 03*, revision B.04; Gaussian, Inc.: Pittsburgh, PA 2003.

(33) Pearson, J. C.; Sastry, K. V. L. N.; Herbst, E.; De Lucia, F. C. *Astrophys. J.* **1997**, *480*, 420.

(34) Hockridge, M. R.; Knight, S. M.; Robertson, E. G.; Simons, J. P.; McCombie, J.; Walker, M. *Phys. Chem. Chem. Phys.* **1999**, *1*, 407.